

The Impact of Polyols on Water Structure in Solution: A Computational Study[†]

Regina Politi, Liel Sapir, and Daniel Harries*

Institute of Chemistry and The Fritz Haber Research Center, The Hebrew University, Jerusalem 91904, Israel

Received: February 3, 2009; Revised Manuscript Received: April 19, 2009

Using molecular dynamics simulations, we study the effect of polyalcohols on water structuring in concentrated solutions, comparing six different polyols that vary in the number of hydroxyl groups and internal structure. For all polyols, we find that the hydrogen bond network order, as assessed by changes in the tetrahedral order parameter, is distorted in the binary solutions as compared with that of pure water and depends on the number of hydroxyl groups and the polyol conformation. While the total number of hydrogen bonds is only slightly reduced relative to that found in pure water, we find that hydrogen bonds that form with polyols tend to be less linear than hydrogen bonds formed between water molecules. We suggest that this reflects the competition between water and polyol molecules for hydrogen bonding with surrounding waters and offer a link between this competition and the resulting disorder that follows polyol solvation. The conclusions of this study should help shed light on the action that polyols can have as stabilizers to other macromolecules such as proteins in solution.

I. Introduction

Beyond their importance as metabolic precursors to many cellular and biologically relevant molecules, polyols (or polyhydric alcohols) also play a central role in cellular osmotic regulation.^{1–3} Polyols, as well as several other solutes of small molecular size, are collectively named “osmolytes” or “compatible cosolutes” because they do not adversely affect the structure and action of the many cytoplasmic macromolecules, even when present at large intracellular concentrations of well over 100 mM.^{3–8} Cells exploit this property and synthesize or accumulate osmolytes in response to high concentrations of harmful solutes, such as salts, in the surrounding milieu. This allows compatible solutes to replace deleterious solutes that the cell, in turn, can transport out of the cytoplasm. Osmotic regulation, therefore, acts to maintain equal water chemical potentials (or water activity) inside and outside of cells while avoiding adverse effects to cellular components.^{3,4,9}

Interestingly, numerous studies show that polyols (such as glycerol and sorbitol) are not only unharmed to cellular macromolecules but that they also tend to thermodynamically stabilize their biologically active state.^{10,11} Proteins, for example, often show higher enzymatic activity and elevated melting temperatures in the presence of these cosolutes.¹² Furthermore, recent studies indicate that polyols, such as inositol, can also correct misfolded proteins and disassemble disease-related protein aggregation such as amyloids.¹³ These effects, together with the sweet taste of polyols, have made these molecules useful as preservatives and stabilizing agents in the pharmaceutical and food industries.¹⁴ However, the molecular property of polyols responsible for their protein-stabilizing effect is still not well resolved.

From a thermodynamic standpoint, the stabilization of proteins (higher ΔG° for unfolding) is directly related to the osmolyte's preferential interaction with the protein.^{2,7,15–19} Simply stated, osmolytes stabilize proteins in their native state

if they are more strongly excluded from the unfolded state than from the native state of a protein. Therefore, the osmolytes' effect depends on the extent to which bulk water serves as a better solvent to osmolytes than water in the vicinity of the protein. The molecular interactions that determine the more favorable solvating environment for osmolytes are diverse. For example, another important osmolyte, trimethylamine *N*-oxide (TMAO), has been shown to prevent protein unfolding by ordering and strengthening water structure while also being shown to be preferentially excluded from the protein's surface.^{20–24} This “structure-making” action of TMAO enhances the penalty associated with protein unfolding and exposure to solution (an increased hydrophobic effect) while at the same time diminishing the ability of water molecules to compete with protein intramolecular hydrogen (H) bonds.

However, in contrast to TMAO, experiments and simulations show that many carbohydrates and polyols seem to interfere with water structure.²⁵ In fact, recent experiments convincingly show little correlation between osmolytes' impact on water structuring in the bulk and their action as protein stabilizers.²⁶ This discrepancy can be reconciled by realizing that any mechanistic description of osmolytes action on macromolecular stability should sensitively depend on both the impact of osmolytes on bulk water and their effect on water in the vicinity of the macromolecule. Therefore, a necessary first step toward determining the stabilizing mechanism of polyols is to study the consequences of their solvation to bulk water.

Here, we describe molecular dynamics (MD) computer simulations of concentrated binary mixtures of different polyols in water and follow the impact of solute addition to water structuring. To find the common important features that give these osmolytes their special properties, we studied six polyols, glycerol, xylitol, adonitol, sorbitol, myo-inositol, and scyllo-inositol. These molecules differ in the number of hydroxyl groups (ranging from 3 to 6) and also in their chemical structure, including linear and cyclic stereoisomers, as shown in Figure 1. Because the term “water structure” is often only loosely defined, we follow here several measures that, taken together,

[†] Part of the “Robert Benny Gerber Festschrift”.

* To whom correspondence should be addressed. E-mail: daniel@fh.huji.ac.il. Fax: +972-2-6513742.

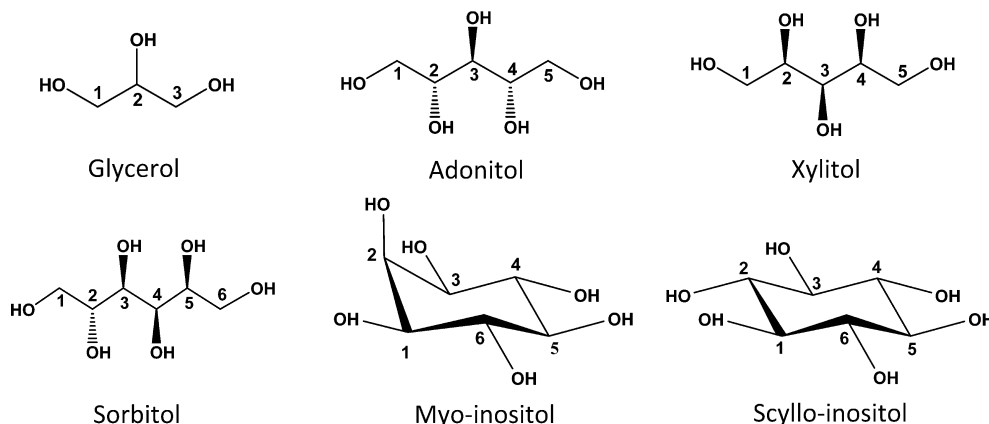


Figure 1. Structure of polyols simulated here: glycerol, adonitol, xylitol, sorbitol, myo-inositol, and scyllo-inositol.

can serve as good indicators of the changes to the H bond network induced by the introduction of osmolytes to solution.

All measures of order that we have studied indicate that water ordering decreases in the presence of high concentrations of polyols, in agreement with experiments^{25,26} and simulations^{14,27} (where available). The extent of water disordering and H bond loss in the presence of solute generally grew with proportion to the number of polyol hydroxyl groups but also depended sensitively on the number of osmolyte internal H bonds, a property that is isomer specific. Interestingly, the formation of more distorted H bonds between water and osmolyte correlated well with a shift toward more linear water–water H bonds in the polyol’s vicinity. This suggests that water binding to osmolyte is less compatible with the water H bond network and that in the presence of osmolytes, the remaining water–water H bonds are optimized while, in concert, the overall network’s tetrahedral structure is diminished.

II. Methods Section

All-atom MD simulations were performed using NAMD.²³ Concentrated solutions of polyols were simulated by inserting 150 solute molecules in a cubic box of 2320 TIP3P water molecules, corresponding to concentrations of approximately 2.4M. All interactions were subject to the CHARMM27 force field^{28,29} and used without further modifications for all polyols. Bonds were kept at a constant length for solutes and solvent molecules. All simulations were performed within the NPT ensemble, at $T = 298$ K (using the Langevin dynamics algorithm as implemented in NAMD) and $P = 1$ bar (maintained using the Nose-Hoover Langevin piston method), within a cubic box with fluctuating length of $L \approx 48$ Å and periodic boundary conditions. After initial energy minimization of 1000 steps and 100 ps of MD equilibration, 20 ns of MD simulation runs were collected, of which only the last 6 ns were used for analysis, with collection steps every 0.5 ps, resulting in well-converged averages for all calculated distributions. The time step in all simulations was 2 fs. Electrostatic calculations were performed using the Ewald particle-mesh summation with 1 Å grid spacing. The van der Waals interactions were truncated smoothly with a cutoff of 12 Å and a switching distance of 10 Å.

MD trajectory analysis was performed using VMD.³⁰ The MD results were compared to several known thermodynamic and experimental solution structural properties for some of the polyols and overall were in close agreement. For example, the experimentally found free energy of hydration for glycerol³¹ (-38.56 kJ/mol) was very close to the value obtained in our simulations by free-energy perturbation as implemented in

NAMD (-43 kJ/mol). In addition, we calculated the Kirwood–Buff integral for sorbitol $G_{SS} = \int (g_{SS} - 1) dV$, where S stands for solute and g_{SS} is the solute–solute pair correlation function, measured as a function of the distance between a central polyol hydroxyl oxygen (O3; see Figure 1) and an osmolyte-representing atom (C3). We found that G_{SS} as evaluated from the simulation gave -0.2 , very close to the previously published experimental value of -0.23 .⁷ The density of sorbitol at 2.4 M as extrapolated from experimental data³² is 1.14 g/cm³. This value differs by 3% from the value found in our simulations (1.11 g/cm³). The experimental density for glycerol solutions at 2.4 M (1.05 g/cm³) is in good agreement with the density value found in our simulations (1.04 g/cm³). We note that for the inositols, the simulated concentrations are in the supersaturated regime.

III. Results and Analysis

Hydration. To assess the extent of osmolyte hydration, we follow the radial distribution functions $g_{sw}(r)$ of water oxygens (denoted W) at a distance r measured from a central representative polyol hydroxyl oxygen (O2 for glycerol and inositol and O3 for the others; see Figure 1). We also follow the extent to which osmolytes are surrounded by other osmolyte molecules as seen in $g_{SS}(r)$, the radial distribution function of osmolytes’ center of mass around the representative hydroxyl oxygen of the central polyol. Figure 2 shows $g_{sw}(r)$ and $g_{SS}(r)$ for all six polyols studied here. We find that these solutes are generally well hydrated, probably because their hydroxyl groups can form H bonds with the solvating water. However, this hydration is significantly different from that of water molecules in pure water.

The function $g_{sw}(r)$ shows two prominent solvation peaks, the first occurring at $r \approx 3$ Å and a second appearing at ~ 5.5 Å. These peaks correspond to waters in the first and second hydration shells and vary with osmolyte size and chemical nature. Table 1 details the average number of water molecules surrounding the polyol hydroxyl oxygen (or “coordination number”), derived by integrating over the first hydration shell in $g_{sw}(r)$ to the first minimum at $r = 3.6$ Å. In general, the coordination number correlates well with polyol size but is also sensitive to the polyol chemical and conformational nature. For example glycerol, a short polyol, has the highest coordination number of 3.02, while the larger polyol, adonitol, is substantially less hydrated with a coordination number of 1.74. Perhaps because glycerol resembles water’s molecular structure to some extent, this polyol’s coordination number is the closest to the corresponding coordination number of pure water, 6.04, reflect-

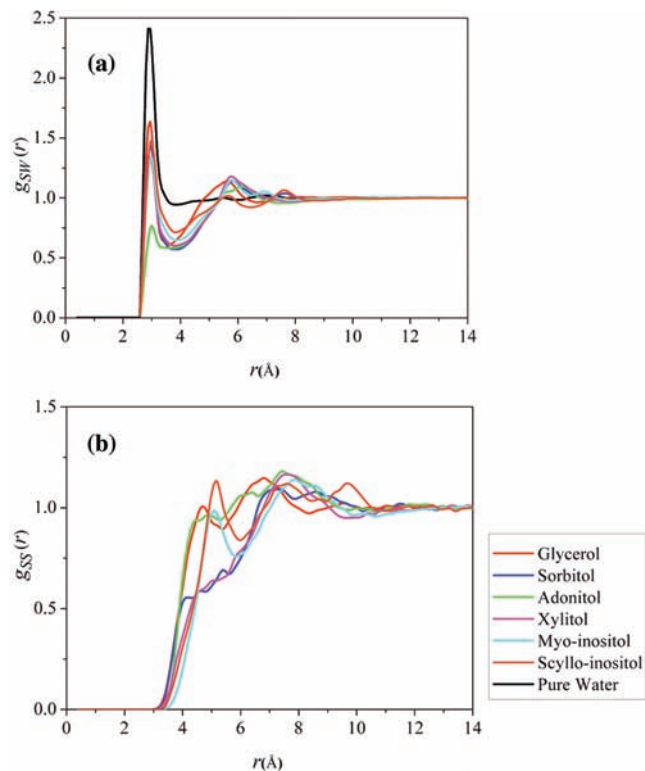


Figure 2. Radial distribution function for (a) water surrounding a polyol molecule $g_{SW}(r)$ and (b) polyols surrounding another polyol molecule $g_{SS}(r)$. Results are shown for six polyols and for water as a reference, color coded as shown in the legend.

ing its preferred hydration. We return to discuss this discrepancy among polyols when we analyze H bonds in the following sections.

The osmolyte radial distribution function $g_{SS}(r)$ shows a first osmolyte–osmolyte correlation peak (or “osmolation”) at around 5–7.5 Å that is further than the first hydration layers, indicating a relative exclusion of one osmolyte from another with respect to water. This peak also corresponds *grosso modo* to a depleted minimum in $g_{SW}(r)$, indicating partial water replacement by polyols in that region.

Water Orientational Order. To determine the effects of polyols on the structural order of neighboring water molecules, we evaluate the tetrahedral structural order parameter, q , a metric that has been used to quantify the tendency of a water molecule and its four nearest neighbors to adopt a tetrahedral arrangement.^{33,34} This measure is defined for the i th water molecule with its four nearest neighbors as

$$q_i = 1 - \frac{3}{8} \sum_{j>k} \left(\cos \psi_{ijk} + \frac{1}{3} \right)^2 \quad (1)$$

where ψ_{ijk} is the angle formed between the central oxygen atom i and two neighboring oxygens j and k (belonging to either water or the polyol hydroxyl group). If oxygens are arranged in a perfect tetrahedral arrangement, $q = 1$, while for an uncorrelated distribution of oxygens, $q = 0$.

Figure 3 shows the probability density of q for pure water and for binary polyol–water solutions. Pure water adopts a bimodal distribution of q values at 25 °C, with a strong peak at $q \approx 0.5$ and a lower “shoulder” at ~ 0.7 . The distribution has previously been attributed to two populations of water molecule ordering in the bulk: one that is more tetrahedrally ordered and another that is less structured.³⁴ Our result somewhat differs from the values reported by Debenedetti et al.^{33,34} that showed

a higher probability for the large ($q \approx 0.7$) peak, even at 30 °C. We ascribe this difference to the water model used in both studies because the modified Toukan and Rahman version of SPC water is known to result in more structured water than the TIP3P potential that we have used.³⁵

For all polyols that we have tested, we find that the binary solutions are less tetrahedrally structured than pure water. Figure 3 shows this polyol effect for three of the osmolytes, glycerol, adonitol, and scyllo-inositol, indicating a decrease in the high q shoulder and an increase and broadening of the low q peak. We also find that for larger polyols, the destructuring effect is stronger. This size-dependent effect suggests that the loss in order could be due to steric (excluded volume) constraints imposed by osmolyte molecules on the surrounding water molecules, as well as to specific hydrogen bonding requirements set by the osmolytes that restrict water’s ability to adopt a perfect tetrahedral arrangement with their nearest neighbors.

We further studied the effect of polyols on the structural order $q(r)$ measured as a function of the distance r from a central solute hydroxyl oxygen using the same definition for r as in $g_{SW}(r)$ above. Figure 4 follows $q(r)$ for the different polyols, clearly showing a lower average value of q for all binary solutions relative to pure water, starting from the polyol vicinity at low r and extending out to the bulk solution. The strong decrease in $q(r)$ values within 6 Å of the polyols indicates that these polyols impose a destructuring effect on their hydrating waters. As also concluded from Figure 3, we find that the larger polyols have a stronger destructuring effect.

While the isomeric pentiols (xylitol and adonitol) do not significantly differ in their influence on q in the bulk, closer to the polyol, the effect of each stereoisomer is distinct, so that adonitol has a stronger destructuring effect than xylitol. We return to discuss the possible reasons for these differences when we analyze H bonding in the following section.

Hydrogen Bonding. There are many possible criteria for defining H bonds in aqueous solutions. To describe the effect of polyols on the H bonding network, we first use one available standard criterion^{36,37} to enumerate the number of hydrogen bonds that are formed or lost upon solute addition. To further analyze the characteristics of the H bonds that are formed, we then dissect the H bond populations in terms of averages and distributions of bond angle and length.

To enumerate H bonds, we define these bonds to exist between two molecules if the oxygen–oxygen distance is less than 3.5 Å and at the same time the $O \cdots O-H$ angle is smaller than $\theta = 30^\circ$, as previously suggested.^{36,37} Figure 5a shows the average number of H bonds per water molecule formed with other waters surrounding it as a function of the distance r from a central solute hydroxyl oxygen, as also defined for $g(r)$ and $q(r)$. In pure water, our model shows that the average number of H bonds per water molecule in the bulk is approximately 3.35. In general, we find that the addition of osmolytes tends to lower the average number of H bonds per water molecule.

For all osmolytes, the average number of polyol–water H bonds per water molecule, Figure 5b, shows a decrease with distance r , with pronounced peaks close to the central osmolyte and also at $r \approx 5.5$ Å. These peaks result from the ability of the polyols to form H bonds with their hydrating waters. Table 1 shows the average number of H bonds that neighboring water molecules form with a central solute hydroxyl oxygen. These numbers correlate well with the water coordination number around the same hydroxyl oxygen, Table 1. The first peak in Figure 5b corresponds to bonds formed with the central osmolyte, while the second closely correlates with waters

TABLE 1: Water Coordination Number around Polyols, Water Hydrogen Bonding to Polyols, and Numbers of Internal and Interpolyol Hydrogen Bonds for Different Polyols

	glycerol	xylitol	adonitol	sorbitol	myo-inositol	scyllo-inositol
water coordination number around polyols ^a	3.02	2.52	1.74	2.41	2.67	2.93
water–polyol hydrogen bonds ^b	1.79	1.30	0.66	1.22	1.16	1.37
number of internal H bonds	0.43	0.66	1.84	1.38	0.0016	0.014
number of interpolyol H bonds	0.42	0.94	0.57	1.11	1.62	1.56

^a Average number of water molecules in the first hydration shell around a representative polyol hydroxyl oxygen atom (O2 for glycerol and inositol and O3 for the others; see Figure 1 and text for details). ^b Average number of H bonds that water forms with a representative polyol hydroxyl oxygen; see text for details.

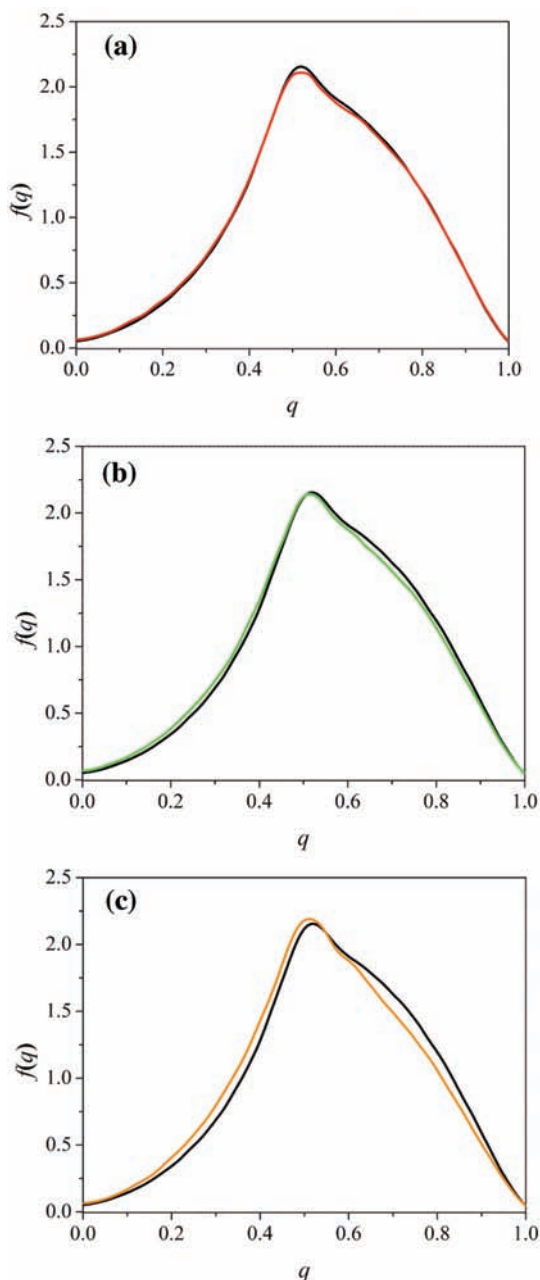


Figure 3. The effect of different polyols on the probability density distribution $f(q)$ of the tetrahedral orientational order parameter q , compared to that of pure water (black line). The probability distribution is shown for glycerol (a), adonitol (b), and scyllo-inositol (c). Colors are as those in the legend of Figure 2.

surrounding the first osmolyte–osmolyte correlation peak (“osmolation”; see Figure 2b), reflecting also H bonds formed with osmolytes accumulated in that shell. We find that the number of H bonds per water molecule that form with other

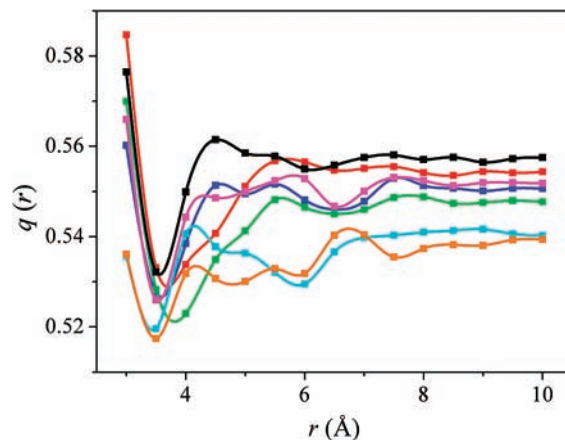


Figure 4. Structural order q as a function of distance r from the polyol, defined as the distance of closest approach to a central polyol hydroxyl oxygen (O2 for glycerol and inositol and O3 for the others; see Figure 1). Colors correspond to the different polyols, as detailed in the legend of Figure 2.

waters surrounding it decreases with osmolyte chain length. Conversely, the smallest number of polyol–water H bonds per water molecule were formed with the shortest osmolyte, glycerol, and generally grew with osmolyte chain length. This balance indicates that lost water–water H bonds are (at least partially) compensated by H bonds formed with osmolytes.

Figure 5c shows the total number of H bonds that a water molecule forms. Interestingly, this total number is very similar for all polyols in the bulk and not much lower than that in pure water, probably reflecting the compensation of one form of H bond by another. Close to the polyols, however, the total loss in H bonding closely follows the loss in H bonds between waters. The modest loss in H bonding, therefore, mainly reflects loss in water–water H bonds that are uncompensated by polyols due to the geometric constraint that these osmolytes pose. For example, compare scyllo- and myo-inositol in Figure 5 and Table 1; scyllo is shown to form more H bonds with water and also allows more water–water H bonds to form. This indicates that by this measure, scyllo-inositol fits into the water H bond network slightly better than myo-inositol (as well as several of the other polyols).

Another important consideration can explain the differences between polyol stereoisomers in their effect on water structure. The number of water H bonds or polyol’s effect on the tetrahedral order $q(r)$ can sensitively depend on the number of internal H bonds that the different isomers can form. Specifically, we find that fewer H bonds form between waters and osmolytes that have a larger number of internal H bonds. Table 1 indicates that adonitol and sorbitol create the largest number of internal hydrogen bonds. Indeed, we find that adonitol is less available to create H bonds with the surrounding water than its stereoisomer xylitol, as reflected in the stronger decrease in the average number of osmolyte–water H bonds in close proximity

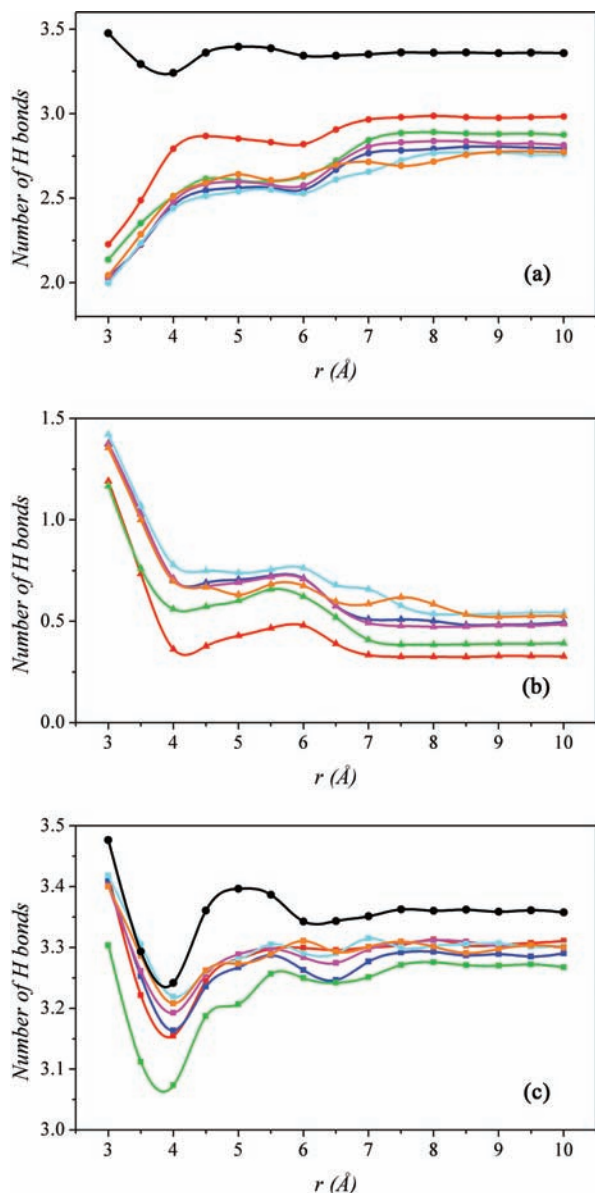


Figure 5. The average number of H bond interactions per water molecule as a function of distance from a central polyol hydroxyl oxygen; see text for details. Panels correspond to water–water H bonds (a); polyol–water H bonds (b); and the average total number of H bonds per water molecule (c). Colors correspond to the different polyols, as detailed in Figure 2.

to adonitol. Similarly, sorbitol that has the same number of hydroxyl groups as scyllo-inositol forms fewer H bonds with water, probably due to its larger number of internal H bonds.

The same tendency is reflected in the interpolyol H bonds, as detailed in Table 1; polyols that tend to form more internal H bonds are less available to form bonds with each other. For example, inositol that forms no internal H bonds creates more interpolyol bonds than sorbitol. Conversely, adonitol, which forms a significant number of internal H bonds, makes fewer interpolyol H bonds than its isomer, xylitol. Moreover, this number is close to that of glycerol, which has only three hydroxyls.

Interestingly, previous studies,²⁷ as well as our own simulations, show that in water, adonitol adopts a planar “zigzag” configuration while xylitol and sorbitol also have a substantial probability of assuming a bent “sickle-shaped” conformation. We suggest that the zigzag structure may impose a stronger

TABLE 2: Average Angles and Distances for Hydrogen Bonds Formed within 5 Å from Any Central Polyol Atom^a

	$\langle\theta_t\rangle$	$\langle\theta_{\text{ww}}\rangle$	$\langle\theta_{\text{ws}}\rangle$	$\langle d\rangle$
water	28.6	28.6		3.012
glycerol	27.7	27.6	29.0	3.004
adonitol	27.9	27.4	32.5	3.005
xylitol	28.1	27.8	30.6	3.006
sorbitol	28.1	27.6	31.8	3.005
scyllo-inositol	29.7	29.0	34.4	3.015
myo-inositol	29.7	29.1	34.0	3.015

^a Subscripts correspond to t, total; WW, water–water H bonds; and WS, water–solute H bonds; see text for details.

disruption to the surrounding water molecules since in this conformation, adonitol prefers internal to water network H bonds and therefore acts as a geometric (steric) constraint that decreases the number of neighboring water–water H bonds close to this “wall”, concomitantly reducing $q(r)$. Finally, on the basis of g_{ws} , we find that the number of water molecules in close proximity to adonitol is small, possibly playing a role in the formation of a relatively small number of H bonds, and in the lower structural order found near adonitol.

We further characterize H bonds found around a given polyol molecule, up to a distance of 5 Å from any polyol atom. We considered the angles θ corresponding to the smallest O...O–H angle between two water–water or water–osmolyte oxygens that were within a cutoff distance of 3.5 Å. These angles were binned for all osmolytes found in a trajectory frame and over 60 frames within 6 ns to produce average and probability distribution functions for θ . In addition, the corresponding oxygen–oxygen distances, d , were measured and averaged. As previously concluded,^{38,39} we have also found that the average $\langle d\rangle$ is an insensitive measure of hydrogen bond character and only slightly differs for the different polyols. We note, however, that the trends seen for $\langle d\rangle$ are generally similar to those that we found for θ , and we return to this point in the Discussion and Summary.

Table 2 indicates that in the presence of all linear polyols, the total mean θ value, $\langle\theta_t\rangle$, slightly decreases with respect to its value in pure water, $\langle\theta_t\rangle = 28.6^\circ$. The smallest $\langle\theta_t\rangle$ value is found for the shortest polyol, glycerol, with $\langle\theta_t\rangle = 27.7^\circ$, while the value closest to that of water is found for the longest linear osmolyte tested, $\langle\theta_t\rangle = 28.1^\circ$ for sorbitol. For the two cyclic osmolytes tested, scyllo- and myo-inositol, we find an increase in $\langle\theta_t\rangle$ with respect to pure water, to 29.7° for both.

With few exceptions, the same trend can be found for the mean θ value for water–water H bonds ($\langle\theta_{\text{ww}}\rangle$). In contrast, we find that the average θ values for osmolyte–water hydrogen bonds ($\langle\theta_{\text{ws}}\rangle$) are higher than the average θ in pure water. The highest $\langle\theta_{\text{ws}}\rangle$ values are found for adonitol and scyllo- and myo-inositol (32.5° , 34.4° , and 34.0° , respectively), indicating, on average, more distorted hydrogen bonds. In fact, these values suggest that many H bonds considered here do not fall into our previous criterion for hydrogen bonds.

A more detailed picture of the structural changes ensued by polyols is revealed by the H bond angle probability distribution. Figure 6 follows this probability distribution, indicating that, as previously demonstrated,³⁸ this distribution in pure water is bimodal, allowing one to clearly distinguish two hydrogen bond populations, a larger population with more tetrahedral or “icelike” structure, peaked at $\theta \approx 12^\circ$, and a smaller population, peaked around $\theta \approx 50^\circ$, which corresponds, according to the studies of Sharp and co-workers,³⁸ to a fifth water molecule forming a highly distorted H bond.

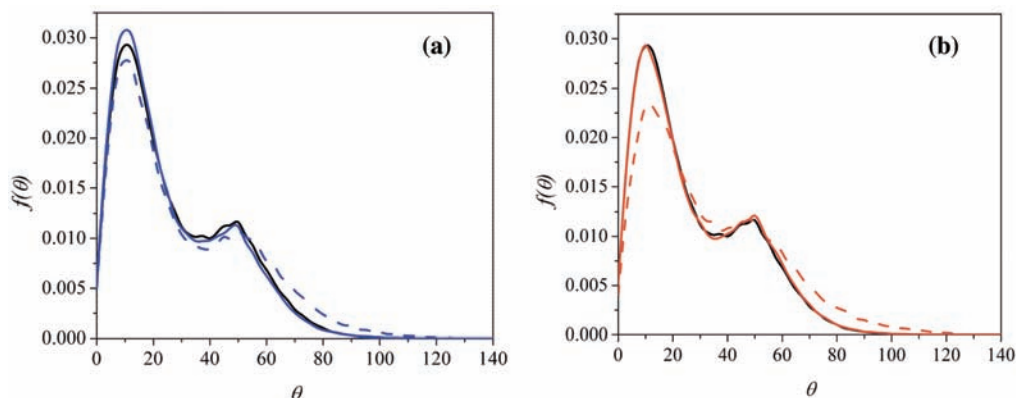


Figure 6. Probability density for H bond contact angles around a polyol. Distributions are shown for sorbitol (a) and scyllo-inositol (b) and compared to distributions for pure water (shown in black). Dashed lines are for polyol–water H bond interactions, and full lines are for water–water H bond contacts.

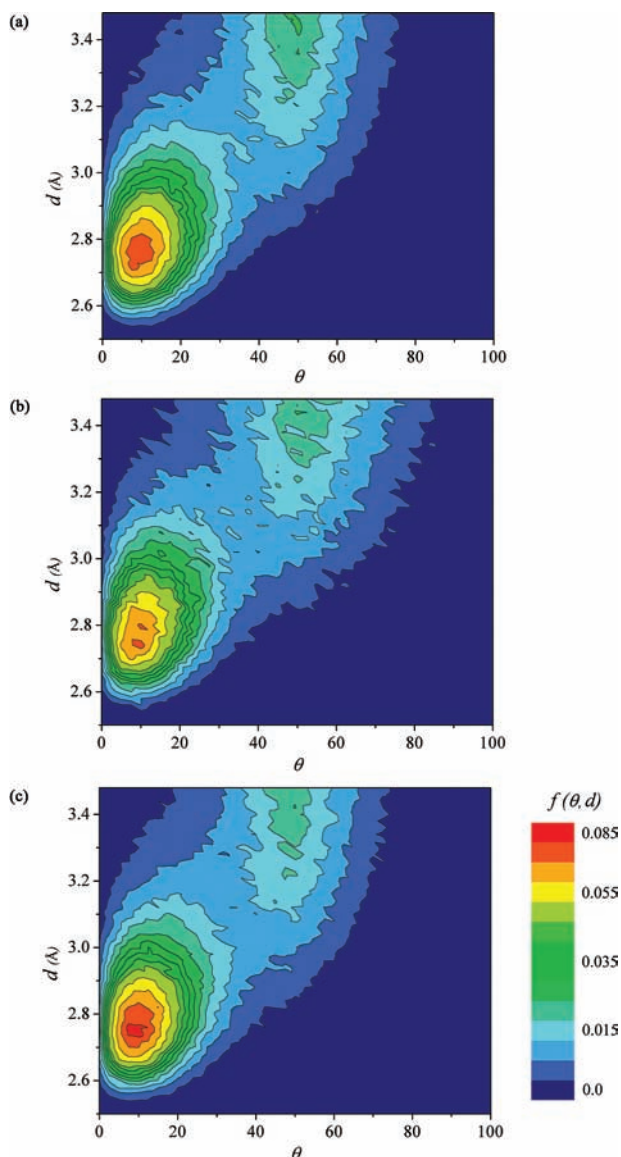


Figure 7. Probability distribution contour plots with respect to the H bond angle and O–O distance for H bonds in pure water (a), for osmolyte–water H bond contacts in an aqueous sorbitol solution (b), and for water–water H bond contacts in the sorbitol solution (c). The color scale shows the probability distribution values.

Figure 6a,b also shows the angle probability for sorbitol and scyllo-inositol aqueous solutions as representatives of the linear

and cyclic polyols. We find that in the presence of polyols, a smaller population of the more linear water–osmolyte H bonds (dashed line in Figure 6) is formed than that in pure water, while we find a larger population of far-from-linear or “strained” H bond contacts. With the exception of the inositols, the larger number of distorted H bonds that water makes with polyols correlates well with an increase in the population of near-linear H bonds that water creates with other water molecules in the hydration shell (full colored line in Figure 6). This suggests that water–polyol interactions that result in distorted H bonds increase the probability to form near-optimal H bonds between available waters in the hydration shell.

These data imply a reorganization of the water H bonding network around polyols, reflected in the order parameter and nature of the H bonds. It is reasonable to assume that H bonds created between water and osmolytes are less preferred than water–water hydrogen bonds, probably due to the smaller polarization of the OH bond in polyols than that in water, as well as the steric constraints imposed by the polyol’s bulkiness, particularly near the nonpolar regions of the molecule. On the basis of our results, we suggest that water molecules in close proximity to osmolytes prefer to forfeit H bonds with osmolytes in order to create more stable hydrogen bonds with neighboring water molecules. In such a way, water’s inability to create optimal H bonds with osmolyte is partially compensated by strengthening the H bond interactions between waters. However, in doing so, the hydrogen bonding network pays in a decrease in order parameter values that reflects a departure from the tetrahedral-like network, as evaluated when all water and polyol hydroxyls are included.

IV. Discussion and Summary

All polyols that we have simulated tend to act similarly in aqueous solutions. We find that for these polyols, the tetrahedral H bonding network ordering is diminished upon osmolyte solvation, depending on the number of hydroxyl groups and conformation (Figures 3 and 4). Interestingly, however, the total number of H bonds that water can form in solution is not much different when comparing pure water and solutions containing osmolytes and is insensitive to the molecular details of the polyol (Figure 5c). This special property is due to the fact that polyols can form H bonds with surrounding waters, so that H bonds lost between waters are, to a large extent, replaced by bonds formed with osmolytes (Figure 5a,b).

Further insights into the balance between H bonds formed with water and those formed with osmolytes is gained when

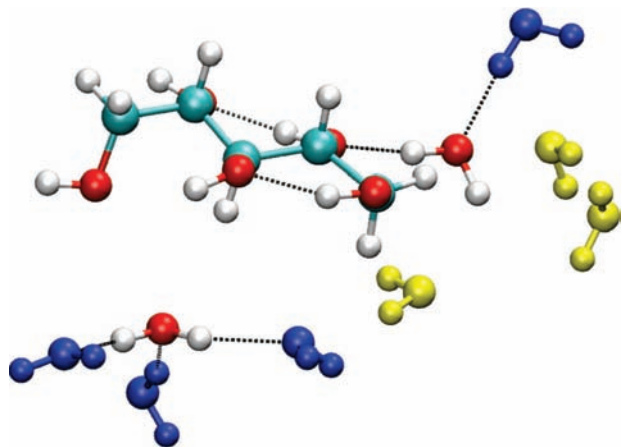


Figure 8. Typical snapshot from MD simulation of adonitol, showing two internal hydrogen bonds for adonitol as well as two contacts to water molecules. In the lower left, the water molecule forms a distorted H bond contact with adonitol but three near-linear H bonds with waters around it (shown in blue). In the upper right, a water molecule forms a near-linear H bond contact with adonitol but only one additional near-linear contact with surrounding water (shown in blue) and several distorted contacts with water molecules (in yellow), and with an additional polyol (not shown).

we dissect H bond contacts by their length and bond angle properties. In the extensive computational studies of Sharp and co-workers,³⁸ it was established that the H bond network in pure water can be separated into two distinct populations. The first contains H bonds that are close to tetrahedral in arrangements, where the typical H bond angle is closer to linear, $\theta \approx 12^\circ$, and has relatively small bond length d . A second, smaller population of H bonds forms distorted H bond angles and shows larger d values. This separation into two populations is well discerned as two separate peaks in Figure 7a, where we show a contour plot of the probability density $f(\theta, d)$ to find H bonds with a specific length and angle, as derived in our simulations.

Furthermore, it was shown that solutes can interrupt this H bonding population in different ways, depending on whether the solutes are polar or nonpolar. Specifically, it was found that nonpolar solutes tend to replace water molecules that form distorted H bonds in pure water, thus allowing waters to form more H bonds that are closer to optimal linear bonds.^{38,39} Conversely, due to electrostatic interactions, polar solutes seem to compete with water's own tendency to make optimal H bonds and tend to increase the nontetrahedral arrangements.

In this respect, polyols are unique intermediate solutes between these extreme cases of nonpolar and polar. We find that while polyols tend to form hydrogen bonds with the surrounding water, they tend to take on the role of the more distorted, suboptimal H bonds in water's H bond network. This can be clearly seen in Figure 7b, showing the H bond contact probabilities for sorbitol in terms of angle and length. The distribution differs from the one of pure water in the widening of the probability for distorted H bonds along the θ axis and the lower probability of H bonds that are close to linear. In concert, H bond contacts in between waters in this binary solution tend to be more linear, as seen in Figure 7c. Figure 8 depicts one typical simulation snapshot with two representative water–osmolyte configurations. The image shows a water molecule forming a distorted H bond contact with adonitol but three water–water H bonds that are almost linear (bottom left of image). We find that for polyols, this type of configuration is statistically favored. Also shown, in upper right of the image, is a water molecule forming an osmolyte–water contact that is

almost linear but only one additional near-linear H bond to a surrounding water molecule, with several distorted H bond contacts to other waters as well as to an additional polyol (not shown, for clarity). This class of configuration is overall disfavored for the polyols.

We conclude that the disruption to the H bonding network in the presence of polyols is minimized by relegating the structure-deforming H bond contacts to water–solute interactions. Thereby, the maximum number of H bond contacts between water molecules can maintain their optimal linear configuration that is commensurate with tetrahedral ordering. This tendency follows from the weaker H bond that can form, even in the most favorable geometry, between osmolyte's hydroxyl and water due to the smaller charge separation of the OH bond in the alcohol as compared to that in water and the geometric constraints imposed by the polyols, probably mostly close to the nonpolar parts of the polyol.

Resolving the effect that polyols have on water structuring in solution should also help in understanding their effect as stabilizers in aqueous solutions of proteins. In particular, it will be interesting to find how polyols act in this stabilizing capacity while generally acting as destabilizers to bulk water, in contrast, for example, to TMAO, and work along these lines is ongoing.

Acknowledgment. We thank Axel Kohlmeyer for his help with VMD programming. The financial support from the Israel science foundation (ISF Grant No. 1011/07) as well as the allocation for a high-performance computer cluster facility (ISF Grant No. 1012/07) are gratefully acknowledged. We also thank the computational support from the Biowulf high-performance computer cluster at the National Institutes of Health during the initial stages of this study. The Fritz Haber research center is supported by the Minerva Foundation, Munich, Germany.

Note Added after ASAP Publication. This paper was published on the Web on May 8, 2009, with typographical errors as well as errors to Figures 4, 5, and 7. The corrected version was reposted on Monday, May 18, 2009.

References and Notes

- (1) Yancey, P. H.; Clark, M. E.; Hand, S. C.; Bowlus, R. D.; Somero, G. N. *Science* **1982**, *217*, 1214.
- (2) Harries, D.; Rösgen, J. A Practical Guide on How Osmolytes Modulate Macromolecular Properties. In *Biophysical Tools for Biologists: Vol 1 in Vitro Techniques*; Elsevier Academic Press Inc: San Diego, CA, 2008; Vol. 84; p 679.
- (3) Hochachka, P. W.; Somero, G. N. *Biochemical Adaptation*; Oxford University Press: New York, 2002.
- (4) Wood, J. M. *Microbiol. Mol. Biol. Rev.* **1999**, *63*, 230.
- (5) Timasheff, S. N. *Annu. Rev. Biophys. Biomol. Struct.* **1993**, *22*, 67.
- (6) Cayley, S.; Record, M. T. *Biochemistry* **2003**, *42*, 12596.
- (7) Rösgen, J. Molecular Basis of Osmolyte Effects on Protein and Metabolites. In *Osmosensing and Osmosignaling*; Elsevier Academic Press Inc: San Diego, CA, 2007; Vol. 428; p 459.
- (8) Auton, M.; Bolen, D. W. Application of the Transfer Model to Understand How Naturally Occurring Osmolytes Affect Protein Stability. In *Osmosensing and Osmosignaling*; Elsevier Academic Press Inc: San Diego, CA, 2007; Vol. 428; p 397.
- (9) Kornblatt, J. A.; Kornblatt, M. J. *Biochim. Et Biophys. Acta* **2002**, *1595*, 30.
- (10) Karsten, U.; Barrow, K. D.; Nixdorf, O.; King, R. J. *Aust. J. Plant Physiol.* **1996**, *23*, 577.
- (11) Chanasattru, W.; Decker, E. A.; McClements, D. J. *Food Hydrocolloids* **2008**, *22*, 1475.
- (12) Haque, I.; Singh, R.; Moosavi-Movahedi, A. A.; Ahmad, F. *Biophys. Chem.* **2005**, *117*, 1.
- (13) McLaurin, J.; Kierstead, M. E.; Brown, M. E.; Hawkes, C. A.; Lambermon, M. H. L.; Phinney, A. L.; Darabie, A. A.; Cousins, J. E.;

French, J. E.; Lan, M. F.; Chen, F. S.; Wong, S. S. N.; Mount, H. T. J.; Fraser, P. E.; Westaway, D.; St George-Hyslop, P. *Nat. Med.* **2006**, *12*, 801.

(14) Carlevaro, M.; Caffarena, E. R.; Grigera, J. R. *Int. J. Biol. Macromol.* **1998**, *23*, 149.

(15) Rösgen, J.; Pettitt, B. M.; Bolen, D. W. *Protein Sci.* **2007**, *16*, 733.

(16) Schurr, J. M.; Rangel, D. P.; Aragon, S. R. *Biophys. J.* **2005**, *89*, 2258.

(17) Auton, M.; Bolen, D. W. *Proc. Natl. Acad. Sci. U.S.A.* **2005**, *102*, 15065.

(18) Timasheff, S. N. *Proc. Natl. Acad. Sci. U.S.A.* **1998**, *95*, 7363.

(19) Parsegian, V. A. Protein–water interactions. *Int. Rev. Cytology* **2002**, *215*, 1.

(20) Zou, Q.; Bennion, B. J.; Daggett, V.; Murphy, K. P. *J. Am. Chem. Soc.* **2002**, *124*, 1192.

(21) Bennion, B. J.; Daggett, V. *Proc. Natl. Acad. Sci. U.S.A.* **2004**, *101*, 6433.

(22) Pincus, D. L.; Hyeon, C.; Thirumalai, D. *J. Am. Chem. Soc.* **2008**, *130*, 7364.

(23) Phillips, J. C.; Braun, R.; Wang, W.; Gumbart, J.; Tajkhorshid, E.; Villa, E.; Chipot, C.; Skeel, R. D.; Kale, L.; Schulten, K. *J. Comput. Chem.* **2005**, *26*, 1781.

(24) Bennion, B. J.; DeMarco, M. L.; Daggett, V. *Biochemistry* **2004**, *43*, 12955.

(25) Dipaola, G.; Belleau, B. *Can. J. Chem.* **1977**, *55*, 3825.

(26) Batchelor, J. D.; Olteanu, A.; Tripathy, A.; Pielak, G. J. *J. Am. Chem. Soc.* **2004**, *126*, 1958.

(27) Grigera, J. R. *J. Chem. Soc., Faraday Trans. 1* **1988**, *84*, 2603.

(28) Brooks, B. R.; Bruccoleri, R. E.; Olafson, B. D.; States, D. J.; Swaminathan, S.; Karplus, M. *J. Comput. Chem.* **1983**, *4*, 187.

(29) MacKerell, A. D.; Bashford, D.; Bellott, M.; Dunbrack, R. L.; Evanseck, J. D.; Field, M. J.; Fischer, S.; Gao, J.; Guo, H.; Ha, S.; Joseph-McCarthy, D.; Kuchnir, L.; Kuczera, K.; Lau, F. T. K.; Mattos, C.; Michnick, S.; Ngo, T.; Nguyen, D. T.; Prodhom, B.; Reiher, W. E.; Roux, B.; Schlenkrich, M.; Smith, J. C.; Stote, R.; Straub, J.; Watanabe, M.; Wiorkiewicz-Kuczera, J.; Yin, D.; Karplus, M. *J. Phys. Chem. B* **1998**, *102*, 3586.

(30) Humphrey, W.; Dalke, A.; Schulten, K. *J. Mol. Graphics* **1996**, *14*, 33.

(31) Marcus, Y. *Phys. Chem. Chem. Phys.* **2000**, *2*, 4891.

(32) Blodgett, M. B.; Ziemer, S. P.; Brown, B. R.; Niederhauser, T. L.; Woolley, E. M. *J. Chem. Thermodyn.* **2007**, *39*, 627.

(33) Lee, S. L.; Debenedetti, P. G.; Errington, J. R. *J. Chem. Phys.* **2005**, *122*.

(34) Errington, J. R.; Debenedetti, P. G. *Nature* **2001**, *409*, 318.

(35) Jorgensen, W. L.; Jenson, C. *J. Comput. Chem.* **1998**, *19*, 1179.

(36) Luzar, A.; Chandler, D. *Phys. Rev. Lett.* **1996**, *76*, 928.

(37) Kumar, R.; Schmidt, J. R.; Skinner, J. L. *J. Chem. Phys.* **2007**, *126*.

(38) Sharp, K. A.; Madan, B. *J. Phys. Chem. B* **1997**, *101*, 4343.

(39) Vanzi, F.; Madan, B.; Sharp, K. *J. Am. Chem. Soc.* **1998**, *120*, 10748.

JP9010026